Power Line Filter Design for Conducted Electromagnetic Interference Using Time-Domain Measurements

Mohit Kumar and Vivek Agarwal, *Senior Member, IEEE*

***Abstract*—A time-domain technique for the design of passive power line conducted electromagnetic interference (EMI) filters in the frequency range 150 kHz–30 MHz is described. A digital storage oscilloscope (DSO) with adequate sampling, storing and processing features is sufficient for the design using the proposed technique. Accordingly, Agilent's Infiniium Oscilloscope (Model 54810A) has been used. The signals from LISN are directly fed into the two channels of the DSO where they are added and subtracted to separate the CM and DM components, thereby eliminating the need for common-mode–differential mode (CM-DM) separator. These components are stored in the DSO. A specially designed filter design software (FDS), residing in the DSO, estimates the noise spectrum by computing the Bartlett and Welch periodograms. It also computes the filter component values. Thus, the sampling of the conducted noise, separation of CM and DM components, signal processing, and filter value computations are all done using one DSO. A spectrum analyzer is not required. Bartlett periodograms have been preferred over Welch periodograms due to low memory storage requirements of the former. The proposed technique has been applied to the design of power line filter for a switched mode power supply (SMPS), and satisfactory results have been obtained. The proposed measurement scheme is compact, economical, and convenient. All the details of this work are presented.**

***Index Terms*—Bartlett and Welch periodogram, common mode (CM), differential mode (DM), electromagnetic interference (EMI), line impedance stabilizing network (LISN), time-domain measurement.**

I. Introduction

CONDUCTED EMI generated by one equipment gets coupled to another equipment mostly through power line cables and can be attenuated (controlled) by using power line EMI filters. Conducted EMI has two components: The common mode (CM) interference and differential mode (DM) interference. The generation and coupling mechanism and the paths of CM interference and DM interference are different and therefore separate filters (CM filter and DM filter) are required to filter (attenuate) them. Both these components of the power line filter can be embedded into a single filter topology as shown in Fig. 1.

The coupled inductor L_c and capacitors C_{y1} and C_{y2} form the CM filter, while the inductors L_D and capacitors C_{X1} and C_{X2} form the DM filter. To design the filters, it is necessary to measure the CM and DM components separately and to obtain their frequency spectrum. Therefore, a CM-DM separator is necessary, which can separate out the two noise components and their frequency spectrum can be obtained. In the past, several techniques have been proposed to separate out the CM and DM components [3], [4].

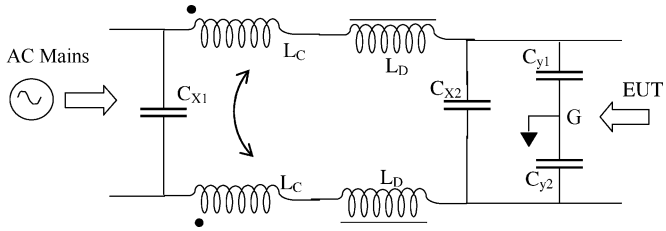

Fig. 1. Power line filter topology for controlling the conducted EMI.

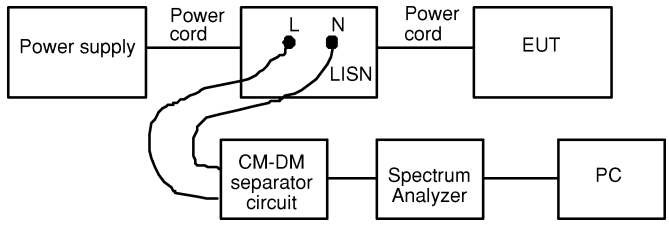

Fig. 2. Conventional setup for the measurement and analysis of conducted EMI.

The output of the CM-DM separator is fed into a spectrum analyzer and the corresponding frequency spectrum is obtained. This data is fed into a personal computer (PC) (typically through a GPIB connection) for further processing and design of the filter components. Shih *et al*. [5] have described a novel filter design procedure. Chang *et al*. [6] have used LabVIEW software for designing the EMI filters. Fig. 2 shows the conventional setup used for displaying the CM interference and DM interference spectrums and designing the filters.

It may be noted that the conventional measurement set-up requires quite a few accessories, namely, an LISN, a CM-DM separator circuit, a spectrum analyzer (SA), GPIB connection, and a PC. Time-domain measurement techniques using digital storage oscilloscopes (DSOs) provide a viable alternative to the conventional method. The conventional method gets particularly tedious when, for example, quasi peak detection needs to be performed.

In the past, a few attempts have been made to apply the time-domain measurement techniques for EMI [7]–[9], but the focus has only been on radiated EMI. Schutte and Karner [7] have compared the time-domain and frequency-domain

Manuscript received December 11, 2004; revised September 22, 2005.

M. Kumar is with the Bhabha Atomic Research Centre, Mumbai, India.

V. Agarwal is with the Department of Electrical Engineering, Indian Institute of Technology Bombay, Powai, Mumbai 400 076, India (e-mail: agarwal@ee.iitb.ac.in).

Digital Object Identifier 10.1109/TEMC.2006.870697

electromagnetic susceptibility testing. The frequency response of simple devices, such as microstrip and coupled microstrip, have been calculated using impulse testing in time domain. The results are identical to those obtained with frequency-domain tests. It shows that time-domain measurements can be used in place of frequency-domain measurements and the former provides a simple, inexpensive, and fast tool of analysis than the latter. Krug and Russer [8] have described a fast measurement technique for radiated EMI, where the noise is sampled in time domain and the corresponding frequency spectrum is obtained by computing the fast Fourier transform (FFT) and the periodograms on a PC. This type of measurement is considered better than the one with a spectrum analyzer because in the former both magnitude and phase information can be obtained. Also, a number of other statistical virtual measurements can be realized using the time-domain sampled data. Krug *et al.* [9] have shown how a time-domain measurement system can be used to simulate the conventional detection equipment, e.g., peak-, average-, RMS-, and quasi-peak-detector through digital signal processing. Some other researchers have also reported time-domain techniques for EMI measurements, but they too deal with radiated noise only. To the best of authors' knowledge, no literature is available which describes time-domain measurement techniques for conducted EMI filter design.

In this paper, a new time-domain technique for the design of EMI filter in the frequency range 150 kHz–30 MHz is proposed. The main objective of this work is to reduce the accessories required for the design of EMI filters, thereby bringing down the efforts and cost and making the system more compact and reliable. As per the proposed scheme, the signals from an LISN (or current probes) are acquired into a DSO having fast sampling, storing, and processing capabilities. The CM and DM components are separated in the DSO using its inbuilt *add* and *subtract* features and are stored in the memory of the oscilloscope as *text* files [10]. The data stored in these $*$.txt files is processed by an especially designed filter design software (FDS), also residing in the oscilloscope. The FDS computes the FFT and the frequency spectrum of CM interference and DM interference components and then goes on to compute the values of filter components as per the algorithm built into the software.

The proposed scheme obviates the need of a CM-DM separator (which is usually a proprietary circuit), a PC for carrying out the necessary computations, an SA for viewing the spectrum of the noise, and the GPIB connection for data transfer. Hence, the proposed measurement setup is more compact and cost effective as compared to the conventional setup depicted in Fig. 2. However, it must be emphasized that the intention is not to replace the existing, conventional EMC test procedures and apparatus with the proposed method, but only to provide a quick and convenient method of designing power line filters.

It must be pointed out that the scope of the proposed technique is not limited to any specific DSO. Any other DSO with a minimum of two input channels, adequate sampling capability, inbuilt math features (e.g., *add* and *subtract*), and sufficient data storage capacity can be used. Since almost all the available DSOs have these features, the proposed scheme is expected to be quite versatile. Because of stiff competition, DSOs with advanced features are now affordable and are generally available in all electronic labs around the globe. The only difference could be that if a DSO does not have inbuilt code compilation and execution facilities (like Agilent's 54810A has), the data can be transferred to a PC through a GPIB cable. Again, PCs are commonly available in all the labs. The main point here is that even a low cost DSO with desired features can be used instead of a costly spectrum analyzer, and the need for a separate CM-DM separator (usually a patented circuit) is obviated.

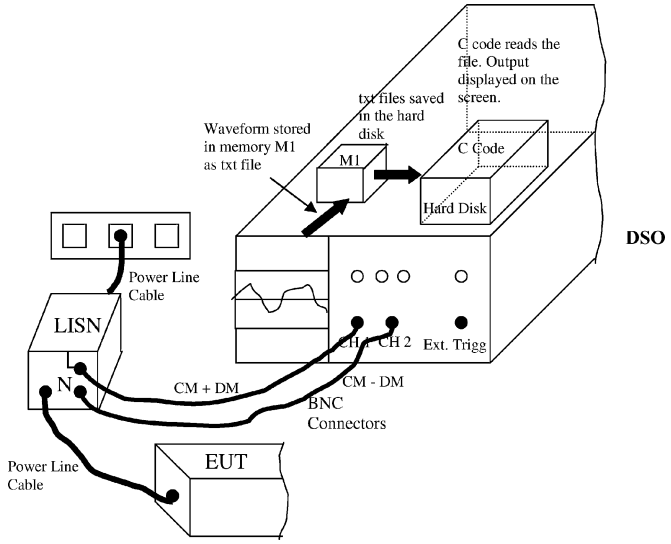

Fig. 3. Block diagram of the time domain EMI measurement system.

The remaining of this paper is organized into the following sections. Section II describes the method and apparatus for the acquisition of noise data using time-domain measurements. Section III presents the details of the computational analysis carried out by the FDS. It includes the frequency spectrum determination using the FFT and the power spectrum estimation using the Bartlett and Welch periodograms. A flowchart of the algorithm used in the FDS and the calculation details required for computing the filter components' values are also described in this section. In Section IV, switched mode power supply (SMPS) examples, based on flyback converter topology, have been considered to demonstrate the design of EMI filters using the proposed technique. Section V presents the major conclusions of this work.

II. Time-Domain Measurements

The proposed time-domain technique makes use of an LISN to sense the line noise. Block diagram of the measurement setup using LISN is shown in Fig. 3. Fig. 4 shows the actual experimental setup. The LISN, fabricated as per CISPR16 standard, is shown towards the right in Fig. 4. The LISN allows the 50 Hz (or 60 Hz) mains supply signal into the EUT without attenuation, but does not allow the noise to go through.

The noise generated by the EUT is filtered and tapped from the LISN's outputs L (line) and N (neutral). The EMI present

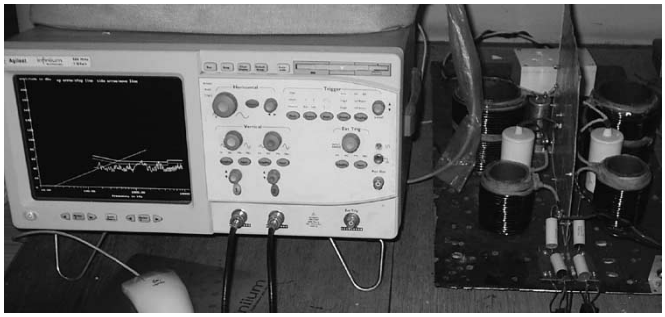

Fig. 4. Experimental setup. The internal circuitry of the LISN is shown on the right side of the DSO.

on the line and neutral phases obeys the following relations:

$$\left.\begin{array}{ll} V_{\rm line} = V_{\rm CM} + \frac{V_{\rm DM}}{2} & \text{(a)} \\ V_{\rm neutral} = V_{\rm CM} - \frac{V_{\rm DM}}{2} & \text{(b)} \end{array}\right\}. \quad (1)$$

The two signals given by (1a) and (1b) are fed into the two channels of the DSO as shown in Fig. 3. The line output of the LISN is fed into channel 1 of the DSO and the neutral output of the LISN is fed into channel 2 of the DSO. The DSO samples the time-domain signals. The inbuilt *add* and *subtract* features of the DSO are used to separate the CM and DM noise. The two channels of the DSO are added and subtracted online to separate the CM and DM noise components as follows:

$$\left.\begin{array}{ll} 2V_{\rm CM} = V_{\rm line} + V_{\rm neutral} & \text{(a)} \\ V_{\rm DM} = V_{\rm line} - V_{\rm neutral} & \text{(b)} \end{array}\right\}. \quad (2)$$

The sampled time-domain CM and DM noise data, after separation, is stored as text files. The advantage of this measurement method is that the separated CM and DM time-domain data is obtained without using a CM-DM separator. This assumes significance considering that the design of CM-DM separator is quite challenging. It has two inputs and they both should be identical to each other to avoid errors due to phase shift. It should be compact and components should be properly mounted to avoid errors due to connections and soldering. To avoid errors due to radiation interference with the CM-DM separator circuit, it is desired to shield it properly. Since EMI extends in the MHz frequency range, good quality magnetic cores are required that can operate at high frequency. The proposed experimental setup eliminates all the problems described above.

A FDS, written in C language resides in the DSO memory. It reads the data as per (2a) and (2b) and processes it using signal processing techniques as described in Section III. This speeds up the filter design process and eliminates the possibility of human error during analysis and computations.

III. Computational Analysis

It is well known that filter design algorithms require frequency-domain analysis of signals. Therefore, in the proposed time-domain technique, the design of power line filters requires the computation of the frequency components of the time-domain signals. The frequency spectrum of a time varying signal is obtained by computing the FFT of the sampled data. In case of noise signal, however, where there is a certain degree of randomness involved, it is more appropriate to compute power spectral distribution of the signal using the Bartlett and Welch periodograms. The FDS designed for this work can compute the FFT or the Bartlett or the Welch periodograms, depending on user's selection.

A. Magnitude and Power Spectrum Using FFT

The frequency spectrum of a time-domain signal is obtained through DFT. The N-point DFT, $X[k]$ of a sequence $x[n]$ of length N is given by

$$X[k] = \sum_{n=0}^{N-1} x[n] e^{-j2\pi kn/N}, \quad 0 \le k \le N-1. \quad (3)$$

FFT of both CM interference and DM interference data (stored as $*$.txt files) is then computed by the software, which gives the magnitude of the voltage $V_{\rm mag}$ in dB. This voltage can be expressed in dBμV using the following relation:

$$V_{\rm mag(dB\mu V)} = V_{\rm mag(dB)} + 120. \quad (4)$$

The voltage spectrum plot is compared with the limit line (imposed by the relevant EMC standard) to compute the attenuation required from the filter. In EMC standards, the *limit line* is usually specified in terms of dBμV, so the magnitude spectrum obtained in (4) is compared with the limit line, which is described as follows:

$$\left.\begin{array}{ll} V_{\rm (CM\,req)dB\mu V} = V_{\rm (CM)dB\mu V} - V_{\rm (Limit)dB\mu V} + 6\ {\rm dB} & \text{(a)} \\ V_{\rm (DM\,req)dB\mu V} = V_{\rm (DM)dB\mu V} - V_{\rm (Limit)dB\mu V} + 6\ {\rm dB} & \text{(b)} \end{array}\right\} \quad (5)$$

where $V_{\rm (CM\,req)dB\mu V}$ and $V_{\rm (DM\,req)dB\mu V}$ is the amount of attenuation required for CM interference and DM interference, respectively; $V_{\rm (CM)dB\mu V}$ and $V_{\rm (DM)dB\mu V}$ is the frequency spectrum of CM interference and DM interference, respectively; and $V_{\rm (Limit)dB\mu V}$ is the limit line as per EMC standards. 6 dB are added to the required attenuation so that the EMI is below the limit line by 6 dB as a factor of safety. From the attenuation plots, the corner frequencies of the CM and DM filters are determined.

In the selected topology the filters are of second order, so the attenuation provided by them is approximated by a 40-dB/decade line. The 40-dB/decade line is drawn by the FDS on the semilog graphical plot. Keyboard is used by the user to slide the 40-dB/decade line along the frequency axis (x-axis) until it is tangent to the interference plot $V_{\rm (CM\,req)dB\mu V}$ given by (5). The horizontal intercept of the line gives the CM filter corner frequency. Similarly, the DM filter corner frequency can be determined from the horizontal intercept of the 40-dB/decade line drawn tangent to the DM attenuation plot. Once the corner frequencies are known, determination of filter component values (L and C) is straight forward.

The power spectrum can be computed from the magnitude spectrum using the following analysis:

$$P = \frac{|V_{\rm mag}|^2}{R} \quad (6)$$

where $V_{\rm mag}$ is the magnitude of the voltage in volts, and R is the resistance in ohms across which the voltage is measured.

Expressing the power in dBμW

$$P_{(\mathrm{dB}\mu\mathrm{W})} = 10\log\left(\frac{|V_{\mathrm{mag}}|^2}{R}\right) + 60\ \mathrm{dB} \tag{7}$$

$$P_{(\mathrm{dB}\mu\mathrm{W})} = V_{\mathrm{mag}(\mathrm{dB}\mu\mathrm{V})} - 60\ \mathrm{dB} - 10\log(R). \tag{8}$$

Since the voltage (noise signal) is measured across the standard 50 Ω resistance, i.e., $R = 50\ \Omega$, therefore

$$P_{(\mathrm{dB}\mu\mathrm{W})} = V_{(\mathrm{dB}\mu\mathrm{V})} - 77\ \mathrm{dB}. \tag{9}$$

All these computations are performed by the developed FDS.

B. Spectrum Estimation From Bartlett and Welch Periodograms

An alternate representation of the frequency spectrum of a time-domain signal can be computed using the Bartlett and Welch periodograms. These periodograms compute the average of the spectrum obtained from the FFT of the time-domain segments of the sampled signal. The spectrum estimation based on a periodogram is a nonparametric method because no assumption is made about how the data was generated [11].

In the Bartlett periodogram, the N-point sequence is subdivided into k nonoverlapping segments, where each segment has length m.

The periodograms for all the k segments are computed and averaged to obtain the Bartlett power spectrum estimate.

$$P_x^P(f) = \frac{1}{k}\sum_{i=0}^{k-1}\frac{1}{m}\left|\sum_{n=0}^{m-1} x_i(n)e^{-j2\pi fn}\right|^2. \tag{10}$$

Bartlett periodogram reduces the frequency resolution by a factor of k. However, the advantage is the reduction in variance by a factor of k. In the computation of the power spectrum using Welch periodogram, the data segments are allowed to overlap. The data segments are windowed prior to computing the periodogram. The periodograms for all the k segments are computed and averaged to obtain the Welch power spectrum estimate.

$$P_{xm}^P(f) = \frac{1}{j}\sum_{i=0}^{j-i}\frac{1}{mu}\left|\sum_{n=0}^{m-1} x_i(n)w(n)e^{-j2\pi fn}\right|^2 \tag{11}$$

where u is the normalization factor for the power in the window function and is given by

$$u = \frac{1}{m}\sum_{n=0}^{m-1} w^2(n). \tag{12}$$

Welch periodogram reduces the variance by a factor of 16 k/5 for a 50% overlap. The advantage of the Welch power spectrum estimate is that the variance is smaller than that obtained with the Bartlett power spectrum estimate.

Broadband time-domain measurement techniques allow emulation of the modes of operation of conventional analog EMI measurement systems, e.g., peak, rms, average, and quasi peak detection [8]. For a formal EMC compliance test, time-domain measurements are not better than the conventional EMI receiver measurements. However, time-domain EMI measurement system, presented in this paper, can be achieved with a commonly available DSO and is both economical and convenient. Further, the time-domain measurements are much faster than the conventional methods as described in [8]. Bartlett or Welch periodograms (average FFTs) can be compared to FFC quasi-peak or CISPR measurements with an accuracy of 3 dB [8].

The proposed time-domain method does not claim to replace the conventional EMI measurement methods for EMC testing of any equipment. The work described in this paper presents a method of capturing EMI using a high end DSO and without using CM-DM separator and computing the EMI spectra using signal processing. The paper describes how signal processing methods can be used for designing a power line filter. The errors involved in the measurement can be taken into account by the FDS, and appropriate margins can be incorporated during the filter design to compensate the errors.

In this work, Bartlett periodograms have been preferred over Welch periodograms as the former requires less memory storage as compared to the latter. Available memory storage may be a critical issue in some DSOs. The Welch periodograms may provide better results but the difference may not be too significant and can be taken care of by keeping appropriate margin in the filter design.

The software computes the spectrum of both CM interference and DM interference and displays it on the DSO screen. The spectrum plot is compared with the limit line and the attenuation plot is computed. From the attenuation plot the corner frequencies for the CM and DM filters are determined and from the corner frequencies the filter component values are determined.

As mentioned earlier, the filter topology used for power line filter can be represented in the form of a second order filter. The bode plot of the CM and DM attenuation is represented by a 40-dB/decade line crossing the x-axis (frequency axis) at the cutoff frequency. Thus, the cutoff frequency is determined from the attenuation plot of the power spectrum of the signal. Fig. 5 shows the flowchart of the software (FDS).

IV. Design Examples

Switched mode power supplies (SPMS) are now being extensively used in space constrained energy efficient applications like hand-held portable equipment, space crafts, missiles, etc., because of their high power to weight/volume ratio. To achieve high power to weight/volume ratio they are operated at high frequencies (typically of the order of tens to hundreds of kilohertz), which brings down the weight and volume of the magnetic components used in these supplies. However, the increased operating frequency leads to an increase in both the conducted and radiated EMI in these systems.

To demonstrate the filter design with the proposed scheme an example is given in which a dual output, flyback-type SMPS (Fig. 6) is considered. The output voltage of the flyback SMPS can be regulated by using "duty ratio control" of the switching power device S1. S1 could be a power MOSFET, an IGBT, or a Bipolar Junction Transistor, depending on the requirements of power and switching speed of the device. As can be verified

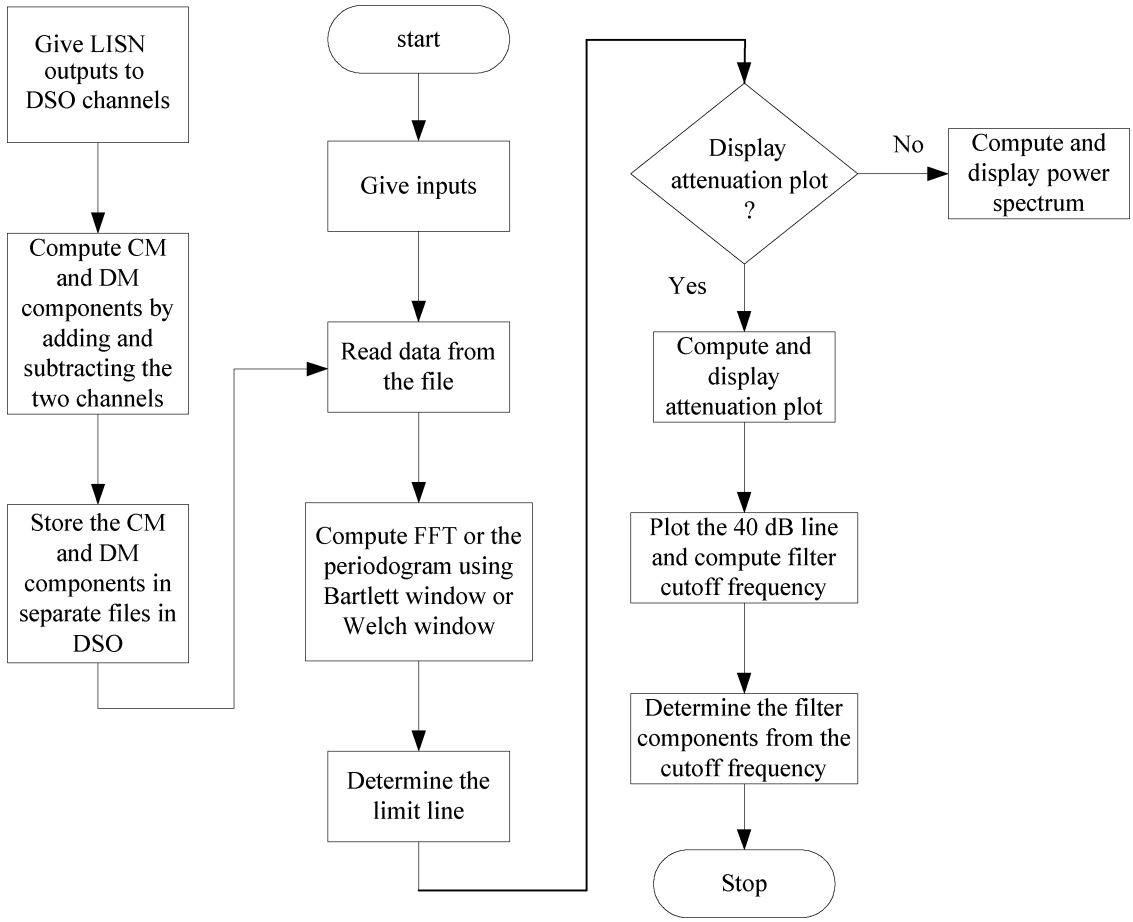

Fig. 5. Flowchart of the software (FDS).

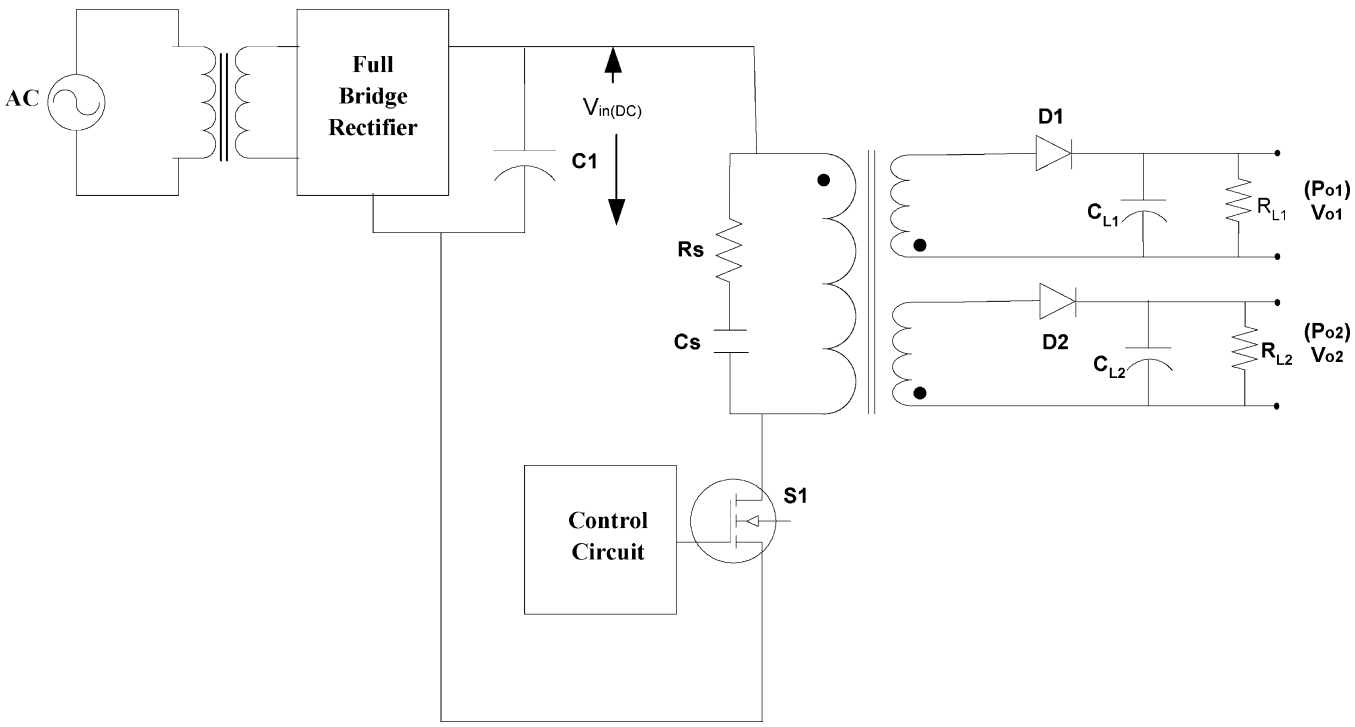

Fig. 6. Schematic diagram of the dual flyback converter.

TABLE I
DUAL-OUTPUT FLYBACK SMPS SPECIFICATIONS FOR THE EXAMPLE CONSIDERED

S. no.	Description	Value
1	$V_{in(DC)}$	70 V
2	f_{switch}	50 kHz
3	$V_{o(1)}$	12 V (DC)
4	$V_{o(2)}$	18 V (DC)
5	$P_{o(1)}$	18 W
6	$P_{o(2)}$	27 W
7	$P_{o(total)}$	45 W
EMI Specifications: CISPR-22		

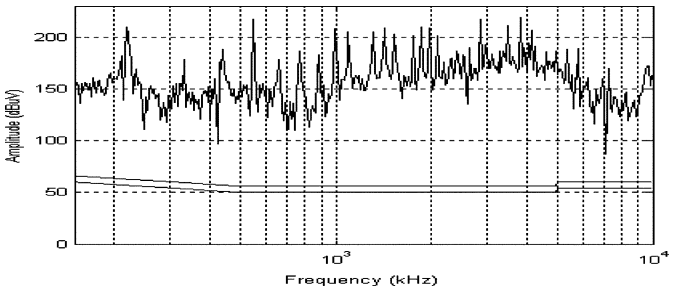

Fig. 7. DM noise spectrum of the SMPS (without EMI filter) computed by the developed software using direct FFT.

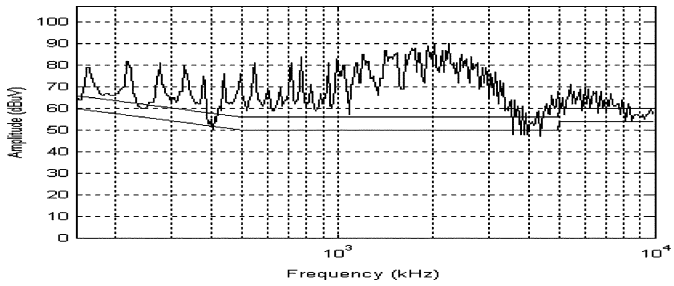

Fig. 8. DM noise spectrum of the SMPS (without EMI filter) computed by the developed software using Bartlett periodogram.

from the "dots" given on the windings of the transformer T1, when S1 is ON, the energy is stored in the inductance of T1. When S1 is OFF, this stored energy is transferred to the output section of the supply. Several paths exist for the CM and DM noise in such a system [12].

Example: A laboratory prototype of a 45-W, dual-output, flyback-type SMPS was built with specifications shown in Table I.

The measurements were performed as per the proposed scheme, to generate the CM interference and DM interference data. The frequency spectrum plots of both the DM interference and the CM interference can be computed by the FDS using direct FFT, as explained in Section III-A or by using Bartlett and/or Welch periodograms, as explained in Section III-B. The DM interference frequency spectrum computed from direct FFT is shown in Fig. 7.

The DM interference spectrums computed using the Bartlett and Welch periodograms are shown in Figs. 8 and 9, respectively.

The nature and trend of EMI in the three spectrums (Figs. 7–9) is close to each other. However, it may be noted that the spectrum obtained in Fig. 7 shows higher values of the components than the spectrums shown in Figs. 8 or 9. It is because no averaging of the data has been done in Fig. 7 while computing the frequency spectrum. On the other hand, the spectrums shown in Figs. 8 and 9 are averaged FFTs. It is more logical to talk about averaged FFT rather than absolute FFT, while referring to noise signals. Therefore, it is important that the filter design is based on Bartlett or Welch periodograms (averaged FFTs) and not absolute FFT.

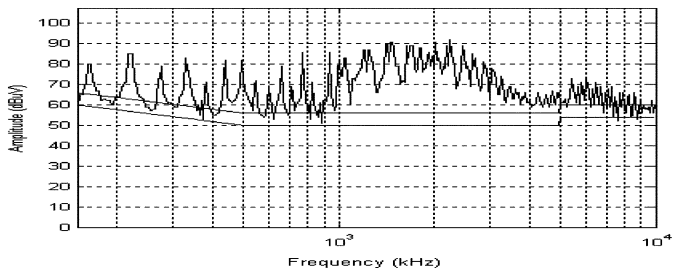

Fig. 9. DM noise spectrum of the SMPS (without EMI filter) computed by the developed software using Welch periodogram.

The CM interference spectrum computed from the Bartlett periodogram is shown in Fig. 10.

An important point to note is that in all the noise spectrums, two limit lines are shown. The upper limit line is the

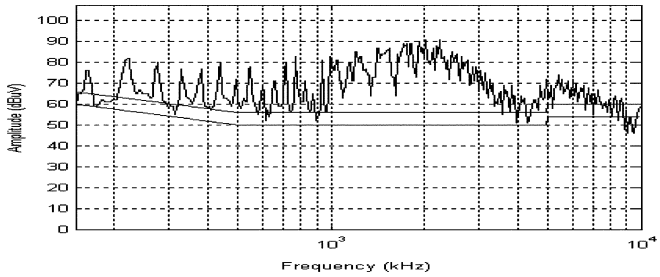

Fig. 10. CM noise spectrum of the SMPS (without EMI filter) computed by the developed software from Bartlett periodogram.

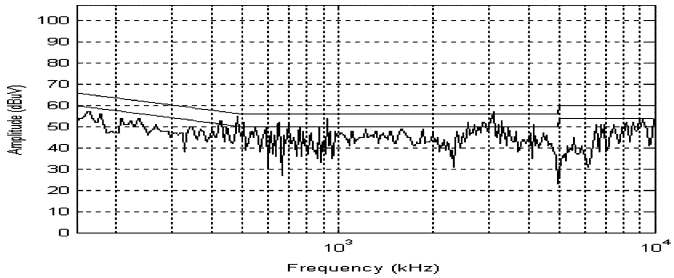

Fig. 11. DM noise spectrum of the SMPS (after incorporation of EMI filter) computed by the developed software using the Bartlett periodogram.

standard limit line as defined in CISPR standard [13]. The lower limit line is 6 dB below the upper limit line. The filter design is done for this lower limit line (and not the actual one), so as to have sufficient margin. It can be seen that DM interference, for the SMPS considered, is above the limit line over the whole frequency range and, hence, requires a power line filter. For determining the filter components' values, Bartlett or Welch periodogram may be considered. Both give nearly similar results. In this work, the former has been used.

Using a 40-dB/decade slope line in Fig. 10, the cutoff frequency for the CM interference spectrum is 47 kHz. It is important to note that the attenuation provided by the second-order filter is 40 dB/decade only under ideal conditions, neglecting the effects of parasitic elements. At high frequencies, the presence of parasitic elements will reduce the attenuation provided by the filter [12].

The CM filter capacitor contributes to the ground leakage current of the equipment in which the filter will be installed. The ground leakage current requirement of the equipment in this work has been taken as 1.0 mA. The value for CM capacitor is computed as follows: If V_p and f are the peak amplitude and frequency, respectively, of the power line voltage and i_g is the ground current requirement of the equipment, where the filter is installed, then the magnitude of the CM capacitor is given by

$$C_y = \frac{i_g}{2\pi f V_p}. \tag{13}$$

However, since there could be a variation in the magnitude of the line voltage by almost 15%, a safety factor $K_{\rm f} = 1.3$ is included in C_y. Therefore

$$\therefore C_y' = \frac{C_y}{K_f}. \tag{14}$$

The values of variables in (13) are $i_g = 1.0$ mA, f (power line frequency) $= 50$ Hz and V (peak voltage) $=$ 314 V. The CM filter capacitance value turns out as $C_y =$ 6082 pF. Equation (14) is used to take into account the effect of voltage variation. The modified CM filter capacitance value is $C_y' \approx 4700$ pF. The CM choke is a source of radiation, so arbitrary large values for CM choke cannot be used. The value for CM choke is given by the equation

$$L_c = \frac{(2\pi f_{\rm CCM})^2}{2C_y'} \tag{15}$$

where $f_{\rm CCM}$ is the CM filter cutoff frequency.

The values of variables in (15) are $f_{\rm CCM} = 47$ kHz and $C_y' \approx$ 4700 pF. The CM filter inductance value turns out to be $L_c =$ 1.2 mH. Since safety has a higher priority than EMI elimination, a smaller value of C_y, and hence a larger value of L_c is used while designing the EMI filter.

The cutoff frequency $f_{\rm CDM}$ for DM interference spectrum given by the FDS is 50 kHz. This is in close agreement with the value obtained with the calculations as shown below.

The DM plot shown in Fig. 8 starts from 150 kHz. EMI level at 160 kHz is 80 dB μV, which exceeds the limit line by 20 dB. So the filter should provide an attenuation of 20 dB at 160 kHz. At $f_{\rm CDM}$, the attenuation provided by the filter is 0 dB. The slope of the attenuation line is 40 dB/decade. Using the equation of a straight line, the following expression can be written:

$$\frac{20({\rm dB})}{\log\left(\frac{160({\rm kHz})}{f_{\rm CDM}({\rm kHz})}\right)} = 40\ ({\rm dB/decade}) \tag{16}$$

which yields $f_{\rm CDM} = 50.59$ kHz ($\approx$50 kHz).

For DM filter, the leakage inductance of the CM choke coil acts as the DM choke coil. The leakage inductance of the CM choke coil was found to be 24 μH, sufficient to eliminate the DM interference. Hence, no additional DM choke coil was added into the circuit. DM capacitors attenuate the 50-Hz line signal, which is not desired. Therefore, arbitrarily chosen large values of DM capacitors cannot be used. The value for DM capacitor is computed as follows. If L_d is the inductance of the DM choke coil, then the value of the DM capacitances is given by

$$C_{X1} = C_{X2} = \frac{(2\pi f_{\rm CDM})^2}{L_d} \tag{17}$$

where $f_{\rm CDM}$ is the DM filter cutoff frequency.

Using $L_d = 24$ μH, the values obtained from (17) are $C_{X1} =$ $C_{X2} \approx 1$ μF.

The DM and CM noise spectrums, after inserting the designed filters, are shown in Figs. 11 and 12, respectively. To compare the performance of the time-domain technique with the conventional technique (using SA), a set of spectrums corresponding to Figs. 8 (or 9) and 10 are given in Fig. 13(a) and (b).

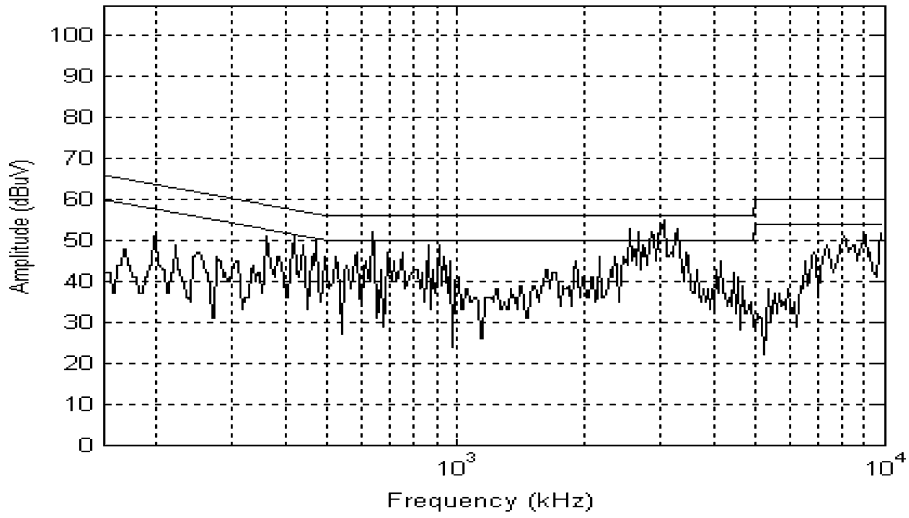

Fig. 12. CM noise spectrum of the SMPS (after incorporation of EMI filter) computed by developed software from Bartlett Periodogram.

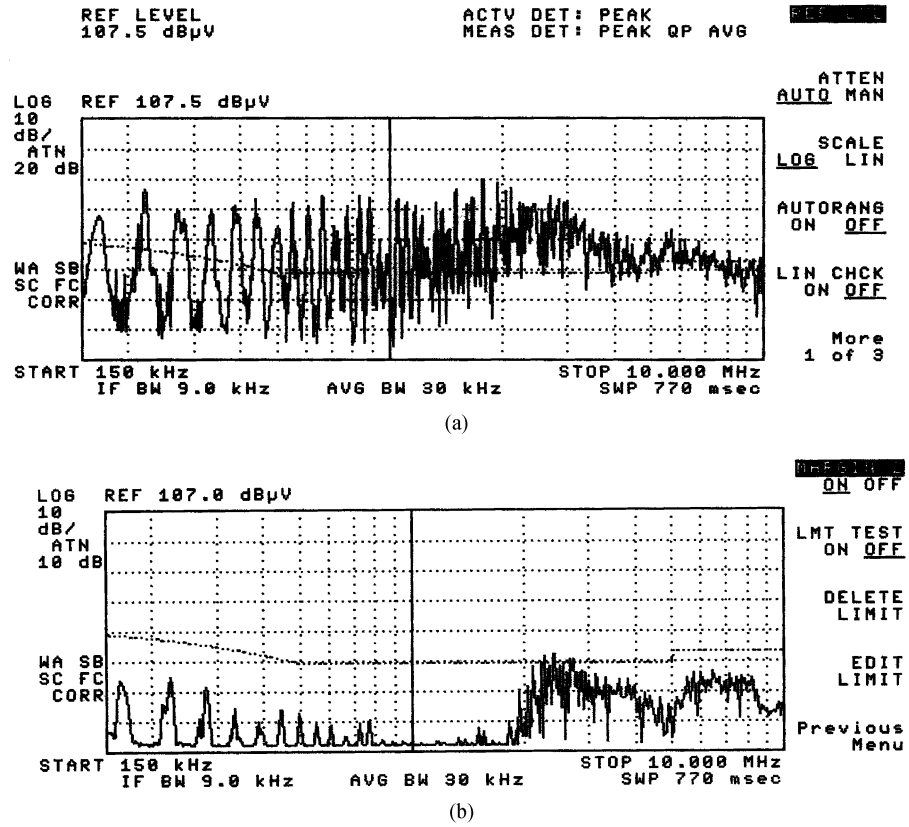

Fig. 13. (a) DM noise spectrum of the SMPS (without EMI filter) obtained from the spectrum analyzer. (b) DM noise spectrum of the SMPS (after incorporation of EMI filter) obtained from the spectrum analyzer.

V. Conclusion

A simple and cost effective EMI filter design technique, based on time-domain measurements, has been presented. Implementation of this scheme requires minimum hardware, obviating the need for expensive equipment such as the spectrum analyzer and proprietary items such as the CM-DM separator. The noise data is acquired, through an LISN, using the inbuilt acquisition power of a DSO. This data is then processed by using the especially designed software (FDS) to predict and display the frequency spectrum of the noise using various algorithms such as FFT, Bartlett and Welch periodograms. It is observed that the use of direct FFT may be misleading in the design of EMI

filters. Instead, Bartlett or Welch periodograms should be used. In the work described here, Bartlett periodogram is considered because the memory requirement is less for computing power spectrum using Bartlett periodogram which could be a crucial issue in some DSO's with limited memory. The frequency spectrum information is then used to design the filter components for CM and DM noise. If a powerful DSO is available, the FDS can reside and execute in the DSO's memory itself. Otherwise, the data from the DSO may be transferred to a PC. This makes the proposed scheme highly versatile, since a PC and high performance DSO is available in almost every electronic laboratory.

Since the data analysis is carried out using software, any amount of signal processing is possible. The signal processing methods can provide an estimate of power spectrum with an accuracy of 3 dB. For example, implementation of the RMS detector, the average detector, and the quasi peak detector is feasible. The statistical analysis of the data is also possible like, for example, the computation of variance in the determination of power spectrum estimate.

The proposed time-domain method does not claim to replace the conventional EMI measurement methods for EMC testing of any equipment. Nevertheless, the paper has described a fast and convenient method of designing power line filters.

REFERENCES

[1] T. Carter, "Switch mode power supplies: An EMI engineer's point of view," Harris Corp., Melbourne, FL, *in Southcon'94. Conf. Record*, pp. 295–300, 1994.

[2] C. Jensen, "Layout Guidelines for Switching Power Supplies," National Semiconductor, Application Note 1149, Oct., 1999.

[3] C. R. Paul and K. B. Hardin, "Diagnosis and reduction of conducted noise emissions," *IEEE Trans. Electromagn. Compat.*, vol. 30, no. 4, pp. 553–560, Nov. 1988.

[4] T. Guo, D. Y. Chen, and F. C. Lee, "Separation of the common-mode- and differential-mode-conducted EMI noise," *IEEE Trans. Power Electron.*, vol. 11, no. 3, pp. 480–488, May 1995.

[5] F.-Y. Shih, D. Y. Chen, Y.-P. Wu, and Y.-T. Chen, "A procedure for designing EMI filters for ac line applications," *IEEE Trans. Power Electron.*, vol. 11, no. 1, pp. 170–181, Jan. 1996.

[6] C. Chang, H. Teng, J. Chen, and H. Chiu, "Computerized conducted EMI filter design system using labVIEW and its application," *Proc. Natl. Sci. Counc. Repub. China A*, vol. 25, no. 3, pp. 185–194, 2001.

[7] A. Schutte and H. C. Karner, "Comparison of time domain and frequency domain electromagnetic susceptibility testing," in *Dig. IEEE Int. Symp. Electromagnetic Compatibility*, Aug. 1994, pp. 64–67.

[8] F. Krug and P. Russer, "The time-domain electromagnetic interference measurement system," *IEEE Trans. Electromagn. Compat.*, vol. 45, no. 2, pp. 330–338, May 2003.

[9] F. Krug, S. Braun, Y. Kishida, and P. Russer, "A novel digital quasi-peak detector for time-domain measurements," in *Proc. 33rd Eur. Microwave Conf.*, Munich, Germany, 2003, pp. 1027–1030.

[10] *Agilent's Infiniium Oscilloscope User's Manual,* Publication 54810-97057, Jan. 2000.

[11] J. G. Proakis and D. G. Manolakis, *Digital Signal Processing Principles, Algorithms, and Applications,* 3rd ed. New Delhi, India: Prentice-Hall, 2002.

[12] J. C. Fluke, *Controlling Conducted Emissions by Design*. New York: Van Nostrand Reinhold, 1991.

[13] *CISPR 22 Information Technology Equipment—Radio Disturbance Characteristics—Limits and Methods of Measurement*, Int. Electrotechni. Commission, IEC, 2003.

Mohit Kumar received the B.S. degree from G.B. Pant University of Agriculture and Technology, Pantnagar, India, and the M.S. degree from the Indian Institute of Technology, Bombay, India, in 2002 and 2004, respectively, both in electrical engineering.

In 2004, he joined Bhabha Atomic Research Centre, Mumbai, India, and is currently working there as a Scientific Officer. His main field of interest is EMI/EMC issues in power supply design and electronic circuits.

Vivek Agarwal (S'94–M'95–M'99–SM'01) received the B.S. degree in physics from St. Stephen's College, Delhi University, New Delhi, India, in 1985, an integrated M.S. degree in electrical engineering from the Indian Institute of Science, Bangalore, India, in 1990, and the Ph.D. degree in electrical engineering from the Department of Electrical and Computer Engineering, University of Victoria, Victoria, BC, Canada, in 1994.

In 1994, he briefly worked for Statpower Technologies, Burnaby, BC, Canada, as a Research Engineer. In 1995, he joined the Department of Electrical Engineering, Indian Institute of Technology, Mumbai, India, where he is currently a Professor. His main field of interest is power electronics. He works on the modeling and simulation of new power converter configurations, intelligent control of power electronic systems, power quality issues, EMI/EMC issues, and conditioning of energy from nonconventional sources.

Dr. Agarwal is a Fellow of IETE and a life member of ISTE.